SLAC-PUB-5734 (Rev.)
April 1993
(T/A)

Oxygen Detection In Thin Silicon Dioxide Layers By Low Energy X-Ray Fluorescence Spectrometry*

Robert E. Kirby

Stanford Linear Accelerator Center

Stanford University, Stanford, CA 94309

David Wherry

Kevex Corporation

355 Shoreway Road, San Carlos, CA 94070

and

Michael Madden

Intel Corporation

3065 Bowers Ave., Santa Clara, CA 95052

Submitted to Journal of Vacuum Science and Technology

* Work supported by Department of Energy contract DE–AC03–76SF00515.

ABSTRACT

Light element detection using low energy (< 2 keV) x-ray fluorescence is described. By tuning the energy of the incident x-rays to slightly above the absorption edge, the minimum detection limits for low-Z elements can be greatly improved over conventional XRF and signal-to-background is significantly better than that obtainable for electron-excited x-ray spectra using an energy-dispersive detector. In particular, the minimum detectable thickness of SiO_2 is experimentally determined to be to be 0.36 Å ($\approx$ 0.1 monolayer) film thickness for 1.85 keV anode voltage using a Mg anode with an Al window. Good signal linearity with film thickness is established by comparsion with measurements obtained on the same samples using ellipsometry and x-ray photoelectron spectroscopy.

I. INTRODUCTION

Bulk x-ray fluorescence (XRF), as an analytical technique, suffers from insensitivity to light elements. The principal cause is that the incident x-rays routinely used to excite the fluorescence spectrum have energies far above the absorption edge of the low-Z elemental line of interest. However, it is exactly the highly penetrating nature of this primary radiation that makes XRF such a valuable bulk analytical tool. The x-ray yields for low-Z element k-lines, and l- and m-lines of higher atomic number elements, though, are very low as a consequence.

If the energy of the primary x-rays is tuned to slightly greater than the absorption edge energy of the elemental level of interest, then a significant improvement in x-ray yield occurs for that line. It is worthwhile to recall here the spectral nature of the the primary radiation emanating from a typical electron-excited anode/filter window x-ray source. The spectrum of x-rays leaving the anode (but not yet intercepted by the window) will contain both characteristic lines (for example, the Mg k-line at 1254 eV) and an underlying broad background of Bremsstrahlung radiation which extends right up to the exciting electron energy. The filter window will act to remove x-rays by absorption, the extent of which is determined by both the window material and its thickness. By carefully choosing anode and window material, as well as window thickness, one can produce a source which, while not monochromatic, can be tailored to optimize the production of certain x-rays in the sample while suppressing those of undesirable components.

In general, the incident x-ray flux is most important in a band of energies just above the energy of the absorption edge of the level we wish to excite. One examines the sample to be probed and searches for an anode that has maximum radiation flux in the appropriate region, whether it be characteristic, Bremsstrahlung or both. A suitable window is then found to maximize transmission of the desirable components of that primary spectrum. If the anode voltage is set too high,

Bremsstrahlung production will shift to higher energy and the intensity of the desired band of incident x-rays decreases. But the higher energy Bremsstrahlung x-rays generated from the source also penetrate more deeply into the sample; consequently, production of low energy x-rays within reach of the surface will decline as well. For example, Figure 1 is a conventional bulk XRF spectrum for Si with a native oxide layer. The O k-line is barely apparent.

Reduction in energy of the primary x-ray spectrum to a few keV, then, results in a decrease in the sampling depth, effectively changing XRF from a bulk to a quasi-surface sensitive technique. It is noted that such an increase in surface and low-Z elemental sensitivity also occurs in electron-excited sample x-ray emission, typically used in the electron microscope because of the ready availability of the electron beam. However, Bremsstrahlung radiation generated in the electron-excited process is responsible for the large backgrounds that reduce the signal-to-background of the detected spectrum and degrade the low-Z detection limit. In the low energy x-ray-excited case, minimal Bremsstrahlung is generated and the signal-to-background is excellent for low-Z elements, as will be demonstrated below, particularly for O.

The question of low-Z elemental fluorescence has been dealt with previously at higher x-ray excitation energies [1]. In the present work, it was our intent to discover the conditions under which the signal can be maximized. These are questions of choice of x-ray anode, anode voltage, and characteristic line versus Bremsstrahlung excitation of the line of interest. Because this technique, low energy x-ray fluorescence (LEXRF), can be surface-sensitive the results can be calibrated using a standard surface-sensitive technique, x-ray photoelectron spectroscopy (XPS).

The possibility of using LEXRF to monitor oxide and nitride thicknesses during semiconductor device manufacture without the need for the vacuum conditions normally required to measure thin films of low-Z compounds makes it a

very attractive technique for cluster tooling [2]. We have chosen to concentrate our yield measurements on the kind of materials that would be encountered under these conditions—Si, SiO_2, and SiO_xN_y.

II. EXPERIMENTS

LEXRF and XPS measurements were made at SLAC in a modified Fisons–VG Scientific, Ltd., Escalab Mark II system [3]. The UHV chamber contained an electrostatic energy analyzer for measuring photoelectron energy distribution spectra (instrumental resolution < 1 eV), an *in situ* selectable dual (Al or Mg) anode x-ray source and an Ar ion sputter gun for sample cleaning. To this system was added a Kevex Inc. [4] energy-dispersive 10 mm^2 x-ray detector with an aluminized (700 Å) BN (3000 Å, 90 wt% B) window ("Quantum") and a second single anode x-ray source from PHI, Inc [5]. It was convenient to change material on the water-cooled PHI source Cu anode end by vacuum deposition in a bell jar evaporator. The sources and detectors could simultaneously view the same point on the sample surface. Angles to the sample surface normal are 50°, 60° and 38° for the Kevex detector, VG and PHI sources, respectively. The area illuminated on the sample by either x-ray source was approximately 1 cm^2.

Samples were loaded and could be sputter-cleaned in a separate load lock chamber. The measurement chamber was ion-pumped and had been previously baked while the unbaked load lock was cryogenically pumped. Typical pressures were 7×10^{-10} and 1×10^{-9} Torr in the measurement and load chambers, respectively. A sketch of the chambers and instrumentation is shown in Figure 2.

The VG source was fitted with a 1 μm Al electron and light filter window. This is not a vacuum window; the source vacuum communicates with the measurement chamber. All Mg and Al anode excitation spectra were taken with

this source. The energy of the emitted x-ray spectrum could be changed electronically by choosing an anode material (characteristic x-rays) and electron bombardment voltage (Bremsstrahlung spectrum). On the PHI source the anode material, electron bombardment voltage and the window material (low-energy x-ray transmission cutoff) were varied. In particular, Cu with a five micron Be window, Cu with a BN ("Quantum") window, and Ta with a BN window were used. The PHI source vacuum was also connected to the chamber vacuum.

The Kevex Si(Li) light-element x-ray detector was fitted with a 10 mm^2 BN entrance window and a magnet electron trap. The trap was enclosed in a magnet-steel stray-field shield to prevent disturbance of photoelectrons generated for the XPS measurements. Light-element x-ray detection capability was confirmed using B metal and the energy resolution was measured on Mn k_α(145 eV). The Si(Li) crystal is cryo-pumped inside the sealed detector tube while the outside of the tube communicates with the measurement chamber vacuum. The detector was checked for the presence of icing using a NaF crystal and comparing the Na/F peak ratio for evidence of the absorption of F x-rays by ice on the detector crystal. None was observed.

Data was taken with these sources down to several hundred anode volts but severe space-charge-limited emission occurs in both sources below about two kilovolts. These sources are designed for use at 15 kV; consequently, space-charge limiting made it impossible to count-rate saturate the x-ray detector for optimum "dead time". The minimum detection limit which depends on signal-to-noise, therefore, was not achieved. Our data is source, not detector, limited. Plotted peak areas presented below are measured after linear background removal. Figure 3 shows the lowest energy k- and l-lines whose detection sensitivities might benefit from tuned x-ray excitation. In the present measurements we concentrated on detecting C,N,O and Si k-lines.

III. SAMPLES

Samples are summarized in Table I. The only sample processed after introduction into the measurement system was native SiO_2 on Si, which we sputter-ion cleaned with Ar to remove the oxide layer in order to determine the ultimate oxygen sensitivity of LEXRF.

IV. DATA

A. Detectability Of O In Thin Si Oxide

A set of well-characterized (by ellipsometry) standards of SiO_2 on Si were available over a considerable thickness range and, therefore, were used to check the signal linearity response of LEXRF for oxygen as well as the ultimate sensitivity for oxygen in Si. We were unable to measure the minimum detection limit (MDL) because of the x-ray sources' inability to saturate the x-ray detector. This is signatured in our data by the presence of a very large noise peak at the left edge of the x-ray spectra.

The VG Mg anode with Al window was used for the linearity and ultimate sensitivity measurements presented in this section. Mg was chosen over Al anode because the characteristic 1254 eV k-line of Mg is closer to the absorption edge of O than the Al 1487 eV k-line. Results comparing anode materials are presented further in this paper. It was found experimentally that an anode voltage of 1.85 keV was ideal for exciting both the Si k-line with Bremsstrahlung and the O k with a combination of Bremsstrahlung and Mg characteristic radiation. The appearance in the spectrum of O and Si k, as well as Mg x-ray scatter from the sample, allows us to compare absolute signals as well as relative ratios of these various components. The stability of the Si intensity was very sensitive to the proximity of the exciting x-ray energy to the Si edge (90 eV difference) and our inability to control the VG anode voltage to better than 10 V. The O peak

intensity (Figure 4), on the other hand, is stable (1300 eV difference, k-line to exciting x-ray energy) and nicely demonstrates the linearity of the LEXRF signal.

The thinnest well-characterized standard available was 82 Å (whose thickness we later measured by XPS to be 83 Å). In order to calibrate with thinner oxides, native SiO_2 on Si was measured for thickness by XPS. All of the standards, native oxide, and partially and fully sputtered native oxide as measured by XPS, are plotted in Figure 5. The points are fitted according to (6):

$$I = I_0 \left[1 - exp(-d/\lambda)\right]$$

where

I = measured XPS oxygen intensity

I_0 = XPS oxygen intensity from an infinitely thick oxide layer

d = film thickness

λ = photoelectron inelastic escape depth

and $I = 0$ at $d = 0$. This standard equation describes the dependance of the photoelectron intensity on film thickness.

The most thoroughly sputter-cleaned Si surface had a remaining XPS SiO_2 film thickness of 0.36 Å. Note that the LEXRF spectrum from this surface (Figure 6) still has usable intensity in the oxygen channel.

B. Choice Of Anode, Anode Voltage, and Window Material

Using a native oxide-covered Si wafer as a test sample, we measured LEXRF spectra using several different anodes and window materials. The oxide thickness was XPS-determined to be 13 Å, initially. The wafer was usually stored in vacuum or in a dry-N_2 storage cabinet between measurements. Due to specimen transfers over an extended time period, the oxide thickness increased somewhat to a final value of 17 Å (determined by XPS) by the last LEXRF measurement. The choice of anode and window was somewhat serendipitous in that the PHI

source uses an anode composed of vacuum-evaporated material on the end of an internally water-cooled Cu tube so that the bare Cu surface was an obvious first anode choice. Combinations of anode and window material were used that maximized, first, the production and throughput of low energy characteristic radiation (Mg and Al, Al and Al, Cu and Be, Cu and BN) and, second, Bremsstrahlung (Ta and BN). These are shown in Figures 7a-e. Comparing these various characteristic line excitations, it's concluded that the O sensitivity is highest for a Cu anode (l-line at 928 eV) and that the throughput at low x-ray energy is best for a BN source window. In no case was it possible to count-rate saturate the x-ray detector.

To investigate the effect of anode voltage (Bremsstrahlung x-ray energy and production rate), we used bulk vitreous C and BN samples, the purpose being to remove sample thickness as a variable. The bombarding electron emission current was held constant as the anode voltage was varied. The flux from the source, however, varies with voltage as does the penetration depth of the Bremsstrahlung into the sample. Figures 8a-c show the results for Cu (strong l-line emission) and Be/BN windows (choice of which affects the low energy Bremsstralung cutoff). To get a better idea of the effect of anode voltage on ultimate sensitivity, Figure 9 shows the intensity/voltage variation for thin native SiO_2 (approximately 13 Å) on Si. Note that x-ray production in the source itself is severely reduced at 1.5 kV anode voltage.

C. Comparison With Electron–Excited X-ray Spectra

Figure 10 shows the strong differences in signal-to-background between electron and tuned x-ray excitation (Figure 7a) for native SiO_2 (13 Å) on Si. The incident electron energy was chosen to include the Si k while maximizing the O k-line. The counting rate for Figure 10 was adjusted to properly saturate the detector. However, the signal-to-background is markedly better in the LEXRF

spectrum, even without saturating the detector. Incidentally, the drop in the Bremsstrahlung at energies just above the O peak in Figure 10 shows clearly the strong x-ray absorption present.

D. Stoichiometric Analysis

Although the agreement on film thickness between LEXRF and ellipsometry is excellent (Figure 4) for an optically well-characterized material like SiO_2, the situation for using optical refractive index as a concentration ratio monitor is distinctly different, e.g., in the case of oxynitrides. The LEXRF N/O counts ratio, determined by peak deconvolution because of peak overlap, and the refractive index as measured by ellipsometry are all listed in Table II for a series of silicon oxynitride films. Also listed is stoichiometric composition of the films as determined by XPS. For thin films, secondary fluorescence and absorption corrections have little effect so one expects the N/O counts ratio in LEXRF to be fairly representative of the actual N/O concentration ratio. Note that two of the films have approximately the same N/O counts ratio but different refractive indicies and two films have the same indicies with different ratios. The LEXRF N/O counts ratio compared to the XPS-determined N/O concentration ratio, however, is self-consistent.

E. Nature of the Primary X-ray Excitation Spectrum

In order to determine the probable shape and relative intensity of the x-ray flux from each of the LEXRF sources used above in Section B, we collected electron-excited x-ray spectra (Figures 11a-d) for samples of Cu, Al, Mg and Ta using 2 keV electron bombardment at fixed beam current. The samples were covered with native oxide and some C contamination. The spectra of Figure 11 essentially represent the output of sources with BN windows (but, in this case, the window is on the detector, not on the source). This is a simple way of

characterizing the output of a source that is best tailored to the excitation of a particular element or group of elements. It would be especially useful for evaluating multi-element sources.

From Figure 11 it is fairly clear why the Cu and Mg anodes are very successful in exciting elemental lines of 500 eV or so. The Cu l and Mg k are sufficiently far below the electron pumping energy for good electron "overvoltage" excitation yet closely above the O k that they are exciting.

V. DISCUSSION

A. Information Depth

This work has dealt with thin Si oxide layers on Si (Figure 4) so that the information depth was determined by film thickness rather than the much larger penetration depth of the primary x-rays. Figure 12 shows the two-thirds x-ray absorption length ($L_{2/3}$) for low energy x-rays in Si with the absorption edges for some lines of interest indicated on the figure. In particular, the O k length is 0.5 μm in Si while that the Mg exciting x-ray used to generate Figure 4 has a penetration of ten times that. It is important to tune the exciting x-ray energy to just above the absorption edge of the element being detected, not only for maximum sensitivity but also minimum information depth, if near-surface analysis is desired. But comparison of Figures 9 and 12 does show that raising the primary x-ray energy above the substrate Si k-edge results in a drop in the O k generation rate. The choice of best anode potential is determined by these competing processes, x-ray generation from the substrate and analyte. In the particular case of SiO_2 films on Si, it seems appropriate to tune the primary x-ray energy to somewhat below the Si absorption edge.

B. Tuned X-Ray Excitation

Figure 7 shows the advantage of using the proper x-ray excitation source for the low-Z analyte region. Storage-ring photon sources are ideal for this because one can change the energy of the characteristic line by using a monochromator, plus the intensity is generally much higher than for lab-based sources. Relatively difficult accessibility makes such a source useful for creating standards but not for routine concentration monitoring.

Another source possibility is illuminating secondary targets with a lab source; however, these targets produce insufficient x-ray flux in the optimum low energy range needed to obtain useful count rates for low-Z analytes.

The voltage (energy) tunable lab source with changeable anodes seems the most practical, particularly if the choice of anode is predetermined using the technique demonstrated in Figure 11. Comparison of Figures 11 and 7 suggests that the choice of anode for low-Z excitation should focus on characteristic line, rather than Bremsstrahlung, production.

C. Potential For Non-Destructive Analysis

The data presented in Section IV, comparing electron- and x-ray excited spectra from native SiO_2, were collected using an energy-dispersive (EDS) detector. It is appropriate to consider how the situation might change using a wavelength-dispersive (WDS) detector with electron excitation. This technique, electron probe microanalysis (EPMA) also shows potential for light-element and thin film analysis [8].

The use of WDS would alter the spectrum of Figure 10. Better WDS energy resolution limits the background, improving the peak-to-background over EDS data collection. However, WDS data collection is tedious for non-repetitive analyses requiring sequential, as opposed to EDS simultaneous, acquisition of peaks.

The higher energy resolution of WDS also makes peak shape an important factor. Integral area-peak factors [8] are needed for each compound of the element for accurate results. Finally, higher-order reflections in WDS spectra may interfere with the lines of interest. Overall, however, it is fair to say that EDS and WDS data collection and processing are competitive for light-element analysis.

EPMA does have a disadvantage in a different way, however, because electron excitation is destructive to thin oxide films. In addition to the potential for beam-induced oxide reduction, electron bombardment of the surface promotes the adsorption of both oxygen- and carbon-containing molecules from the gas phase, changing the very nature of the surface while the data is being collected.

In the Introduction, the possibility was raised of using LEXRF for monitoring semiconductor oxide thicknesses during manufacturing. Using a vacuum-sealed Cu anode LEXRF source with a BN window would make such analyses possible in a reduced-pressure He atmosphere, eliminating the need to analyze semiconductor devices in high vacuum. Such technology would be attractive for cluster-tool architecture [2]. It is the non-destructive potential of LEXRF that makes it attractive for thin film analysis.

VI. CONCLUSION

We have demonstrated the ability of LEXRF to measure extremely thin native oxides of Si. The oxygen signal is linear with thickness and, by using XPS and ellipsometry, the sensitivity can be calibrated. Measurement on Si oxynitrides also suggest that LEXRF has good potential for measuring stoichiometry, as opposed to ellipsometry which is the most common nondestructive technique now used for this purpose. Further work is needed on improving the brightness of sealed, preferably multi-anode, low energy x-ray sources.

REFERENCES

1. R. G. Musket, X–Ray Spectrometry **19**, (1990) 185.
2. T. K. McNab, Semiconductor Int. **13**, No. 9 (1990) 58.
3. Fisons–VG Scientific, Ltd., East Grinstead, Sussex, UK.
4. Delta Level III, Fisons–Kevex, Inc., San Carlos, CA 94070.
5. Perkin–Elmer Corp., Physical Electronics Division, Eden Prairie, MN 55344.
6. C. S. Fadley, J. Electron Spec. Rel. Phenom. **5**, (1974) 725.
7. Data plotted from: B. L. Henke, P. Lee, T. J. Tanaka, R. L. Shimabukuro and B. K. Fujikawa, Atomic Data and Nuclear Data Tables **27**, 1 (1982).
8. G. F. Bastin and H. J. M. Heijligers, Microbeam Anal. **1**, 61 (1992).

TABLE I. Samples

Sample	Description	
Native SiO_2, several pieces	Air-oxidized to ~ 15 Å on Si; characterized *in situ* by XPS. Some samples were Ar ion-sputtered *in situ* to smaller thickness.	
SiO_2 layers on Si	Thickness (82, 100, 115, 330, 557 Å) measured by ellipsometry.	
Vitreous C	Evaporation crucible bottom.	
BN	Hot-pressed, type HP, Carborundum Corp.	
SiO_xN_y	Prepared by CVD. Thickness (d) and refractive index (RI) measured by ellipsometry.	
	d = 1.1450 μm	RI = 1.7712
	= 1.1230 μm	= 1.7600
	= 0.7610 μm	= 1.6395
	= 0.7897 μm	= 1.7545

TABLE II. Silicon Nitride Stoichiometric Analyses

Compound	XPS N/O	Refractive Index	LEXRF N/O
$SiO_{1.43} N_{0.49}$	0.340	1.7545	0.422
$SiO_{1.55} N_{0.55}$	0.356	1.6395	0.403
$SiO_{1.22} N_{0.76}$	0.625	1.7600	1.113
$SiO_{1.18} N_{0.78}$	0.661	1.7712	1.116

LEXRF data taken with Mg anode at 2.0 kV, Al window.

FIGURE CAPTIONS

1. Bulk XRF spectrum, 15 Å native oxide layer on Si. Al anode at 15 kV, Al x-ray source window, 100 s counting time.
2. Experimental system containing x-ray, electron and ion sources and detectors for LEXRF and XPS.
3. Low energy k and l x-ray lines with energies below 1 keV.
4. LEXRF O k-line intensity versus thickness (determined by ellipsometry and XPS). Mg anode, 1.85 kV, Al x-ray source window, 500 s counting time. Line equation: $I = 111.8d + 1668.7$. One $\sigma = 116$ cts at 115 Å. Linear correlation coefficient (r)=0.997.
5. XPS O intensity plotted against thickness determined by ellipsometry for values ≥ 80 Å and XPS for native oxides. The inelastic escape depth for O photoelectrons in SiO_2 is 13.8 Å.
6. LEXRF spectrum of Ar ion-sputter cleaned Si. Remaining equivalent SiO_2 thickness determined by XPS = 0.36 Å. Mg anode at 1.85 kV, Al window, 500 s.
7. Spectra of native oxide on Si (thickness range, 13 to 17 Å) for different anode/window combinations. Counting time is 300 s for a, b, and c, and 500 s for d and e.
   (a) Mg anode at 1.85 kV, Al window; full scale = 865 counts;
   (b) Al anode at 1.85 kV, Al window; full scale = 621 counts;
   (c) Cu anode at 1.90 kV, 5 μ Be window; full scale = 3304 counts;
   (d) Cu anode at 1.85 kV, BN ("Quantum") window; full scale = 140 counts;
   (e) Ta anode at 1.85 kV, BN window; full scale = 2061 counts.

8. Carbon, N and O spectral intensities from bulk vitreous carbon and solid BN for varying anode potentials from 0.5 to 2.0 kV, Cu anode.

   (a) carbon sample, BN and Be windows;

   (b) BN sample, BN window;

   (c) BN sample, Be window.

9. Oxygen and Si spectral intensities from thin (13 Å) native SiO_2 on Si for varying anode potentials from 1.5 to 2.0 kV, Mg anode, Al window. The Si k x-ray absorption edge is 1.84 keV.

10. Electron-excited (2 keV) spectrum of native SiO_2 on Si, optimized for O/Si intensity ratio. Note the large background at low energy, compared to Figure 7a. 100 s counting time, full scale = 3677 counts.

11. Electron-excited x-ray spectrum of air-oxidized anode source materials at 2 keV, 22 nA electron beam current, 100 s. These correspond to x-ray source spectra with BN filter windows (the material used on our detector).

    (a) Mg, (b) Al, (c) Cu, (d) Ta.

    The Mg intensity is reduced by a thick surface oxide.

12. Two-thirds x-ray absorption length, $L_{2/3}$, versus x-ray energy for Si. The absorption edges of a few low energy lines of interest are indicated on the figure.

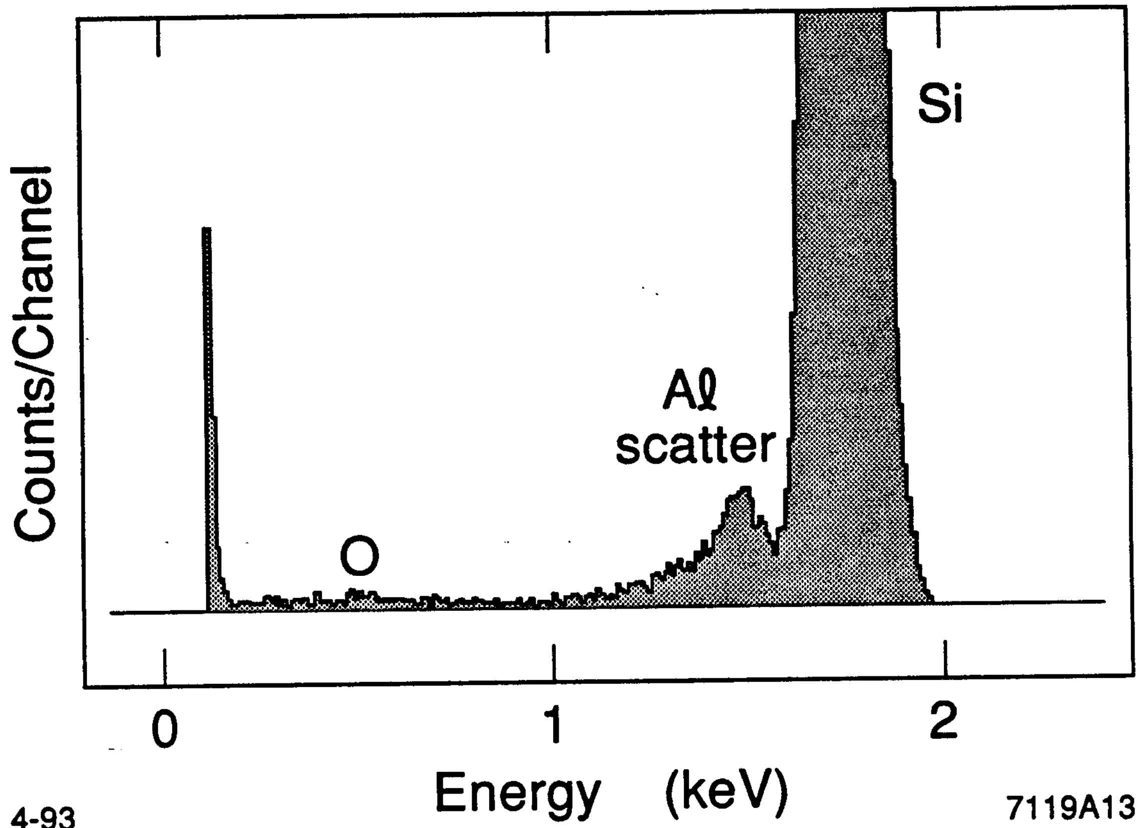
Si
Aℓ
scatter
O
Counts/Channel
0
1
2
Energy (keV)
4-93
7119A13

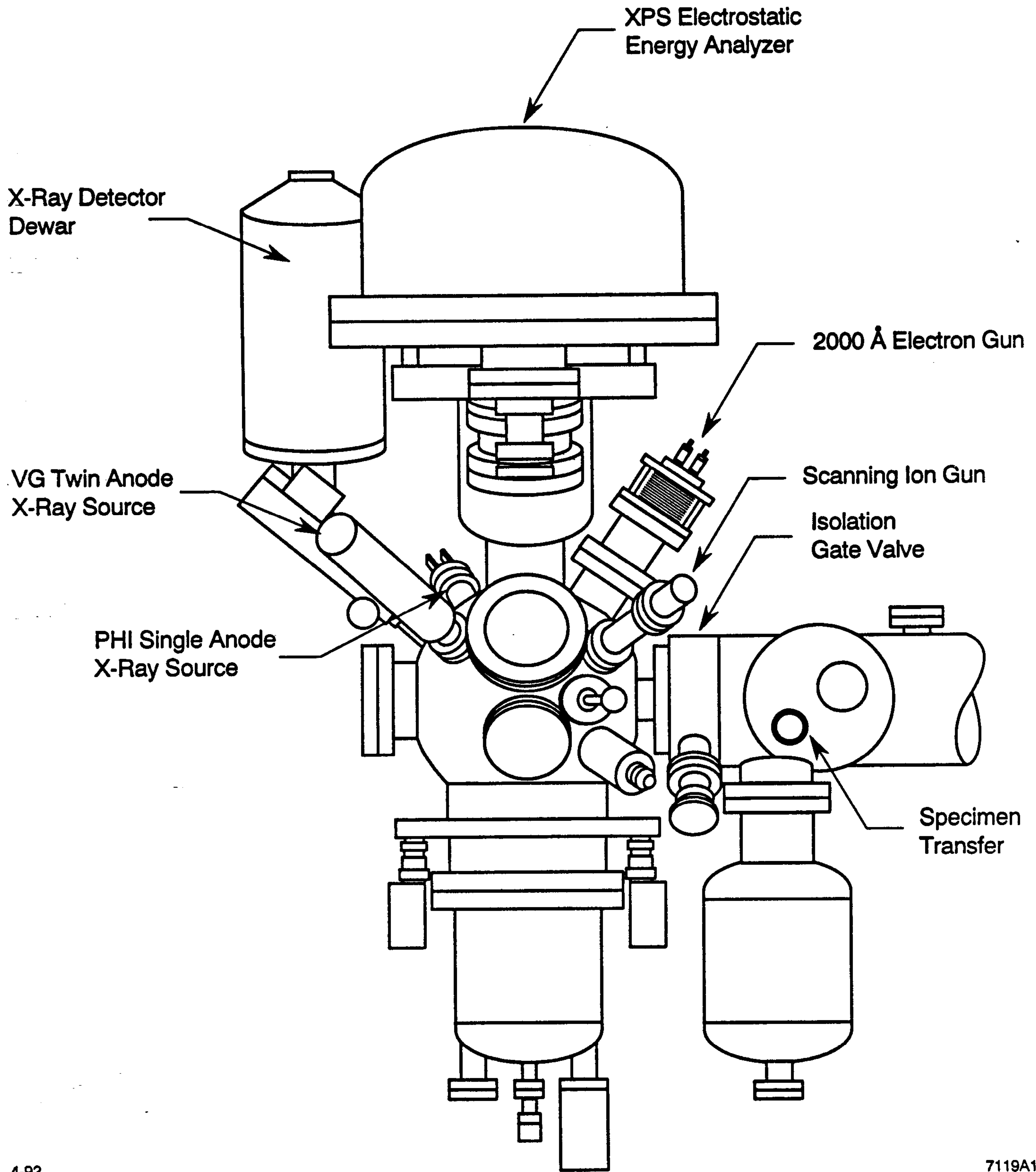
XPS Electrostatic
Energy Analyzer
X-Ray Detector
Dewar
2000 Å Electron Gun
VG Twin Anode
X-Ray Source
Scanning Ion Gun
Isolation
Gate Valve
PHI Single Anode
X-Ray Source
Specimen
Transfer
4-92
7119A1

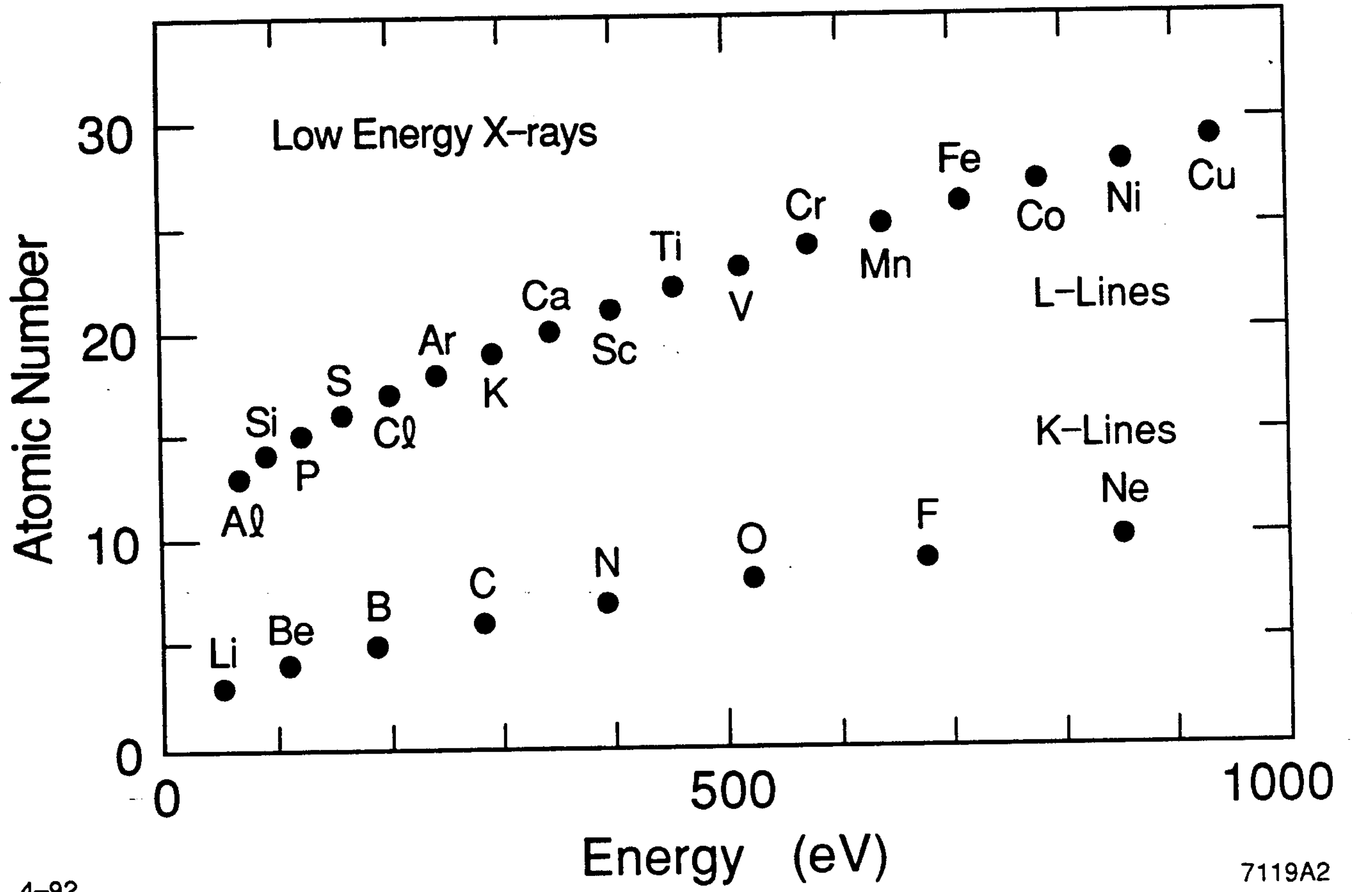

Low Energy X-rays
Atomic Number
Energy (eV)
L-Lines
K-Lines
0
10
20
30
0
500
1000
Li
Be
B
C
N
O
F
Ne
Aℓ
Si
P
S
Cℓ
Ar
K
Ca
Sc
Ti
V
Cr
Mn
Fe
Co
Ni
Cu
4-92
7119A2

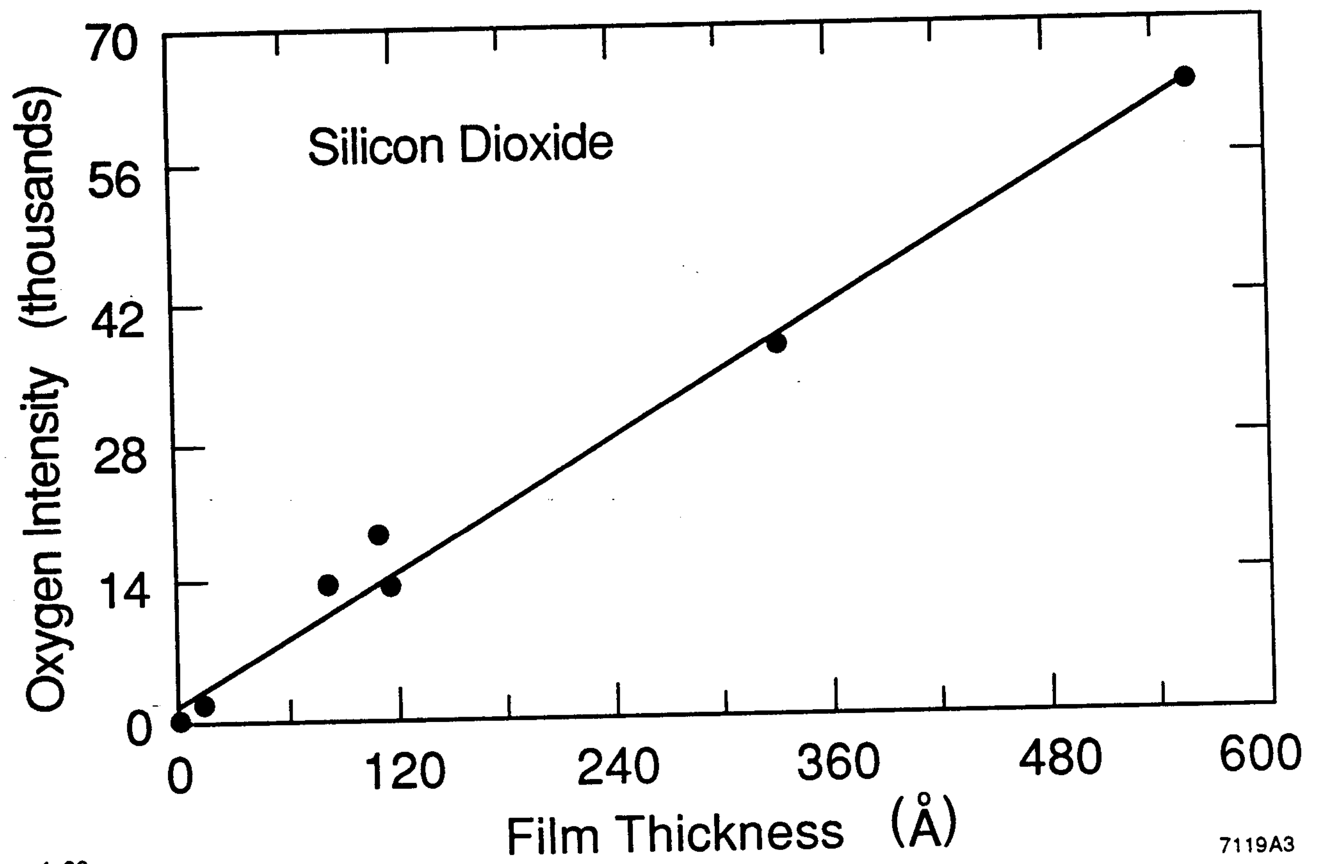
Silicon Dioxide
Oxygen Intensity (thousands)
70
56
42
28
14
0
0
120
240
360
480
600
Film Thickness (Å)
7119A3
4–92

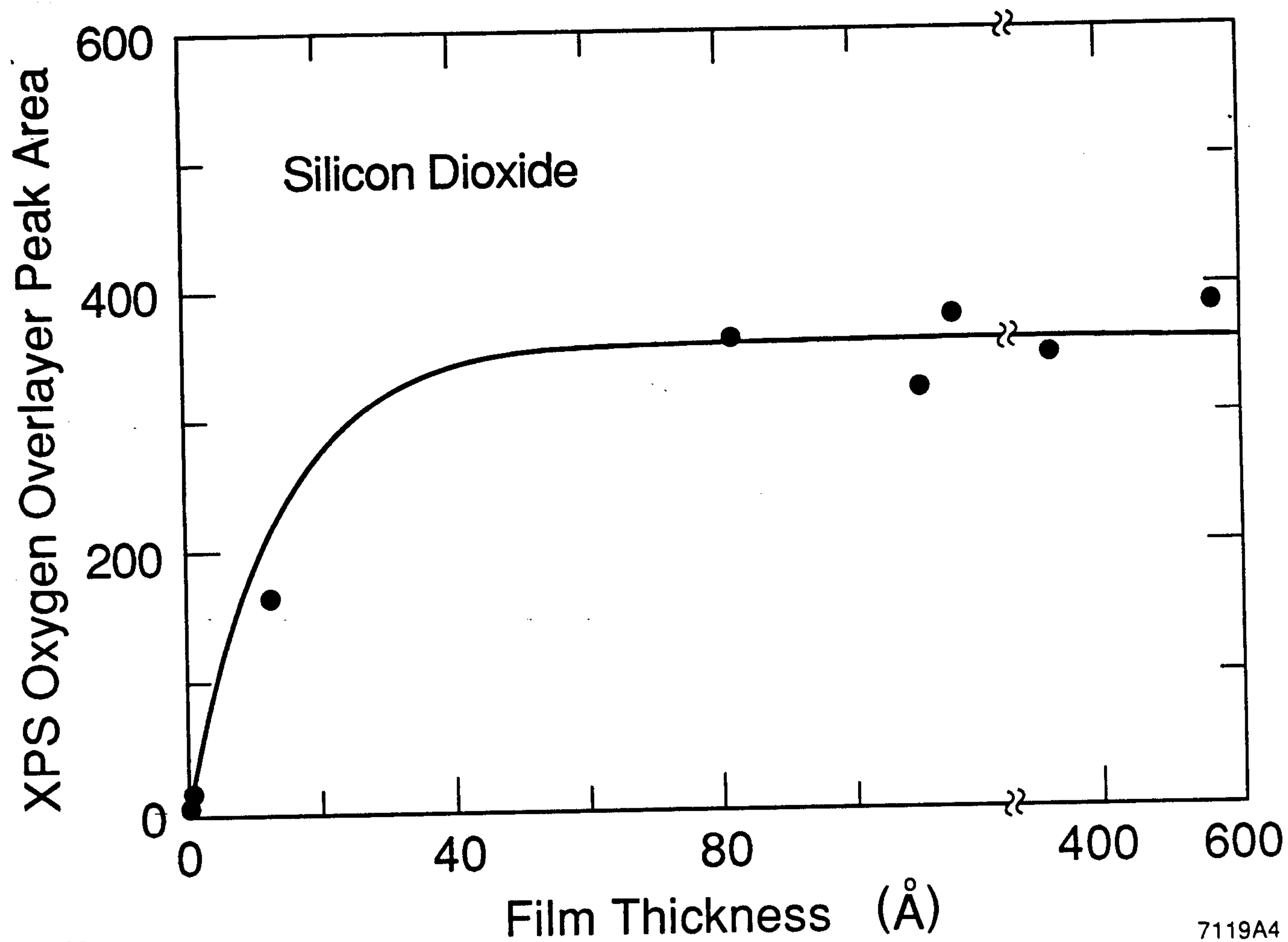

Silicon Dioxide
XPS Oxygen Overlayer Peak Area
600
400
200
0
0
40
80
400
600
Film Thickness (Å)
4–92
7119A4

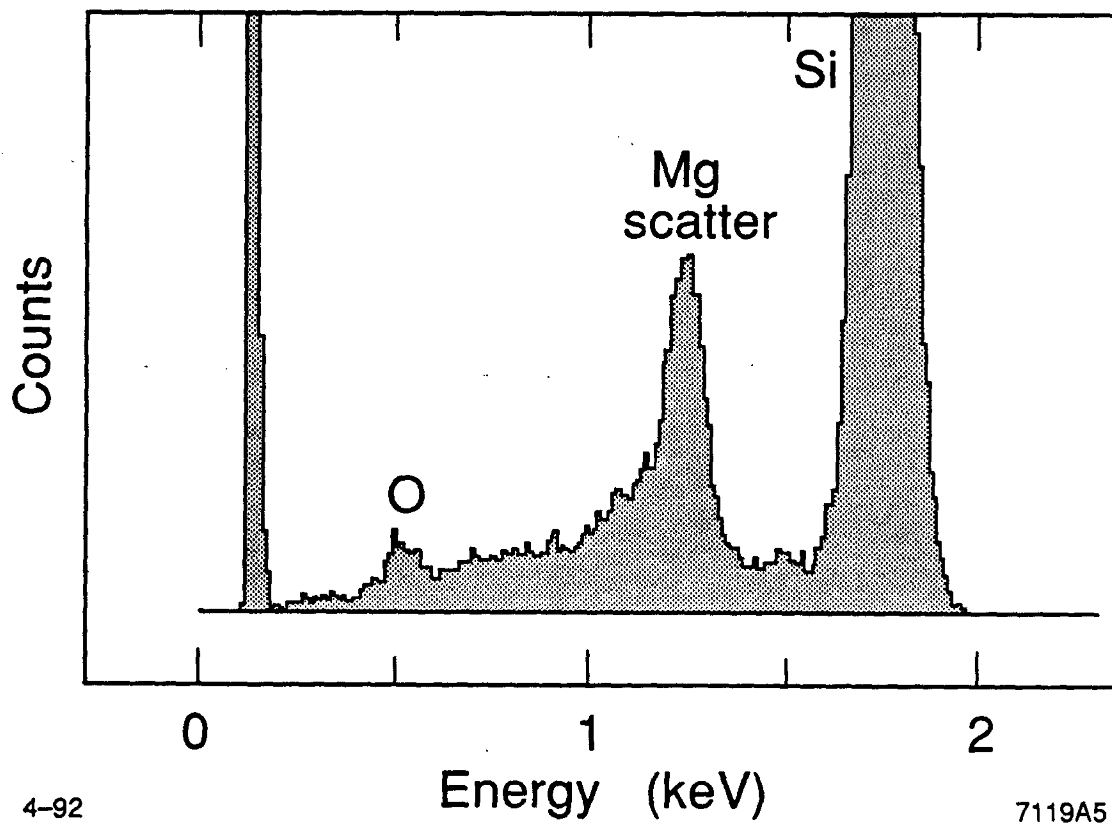
Si
Mg
scatter
O
Counts
0
1
2
Energy (keV)
4–92
7119A5

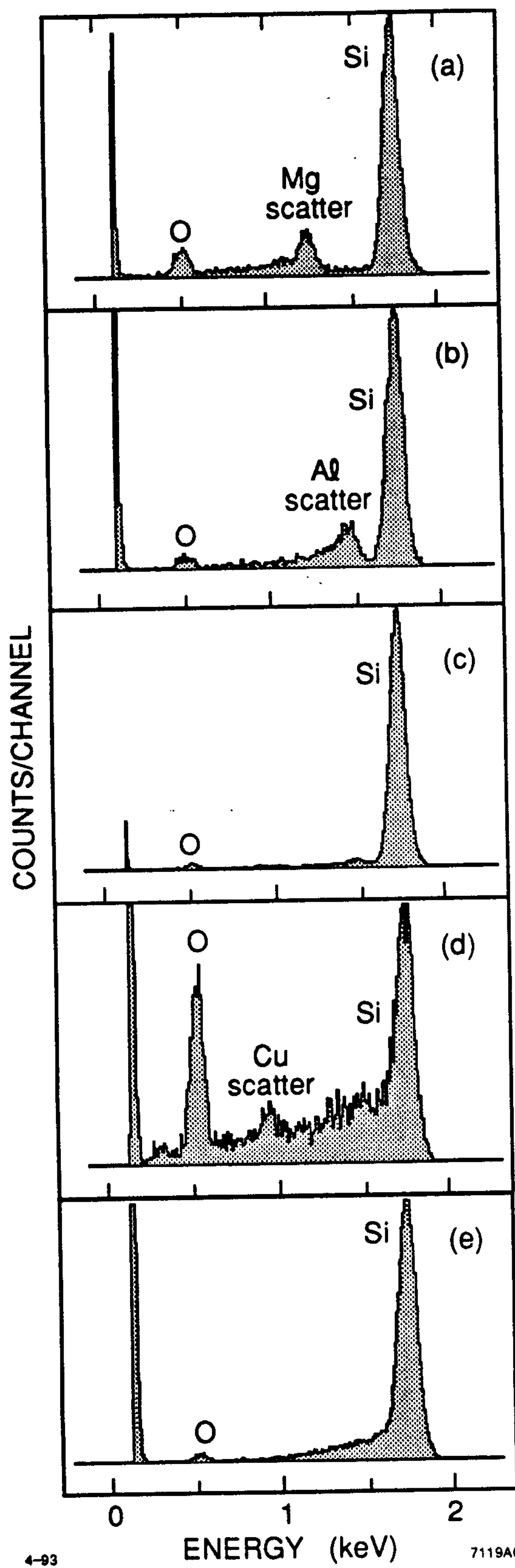

Si
(a)
Mg
scatter
O
(b)
Si
Al
scatter
O
(c)
Si
O
COUNTS/CHANNEL
(d)
O
Si
Cu
scatter
Si
(e)
O
0
1
2
ENERGY (keV)
4-93
7119A6

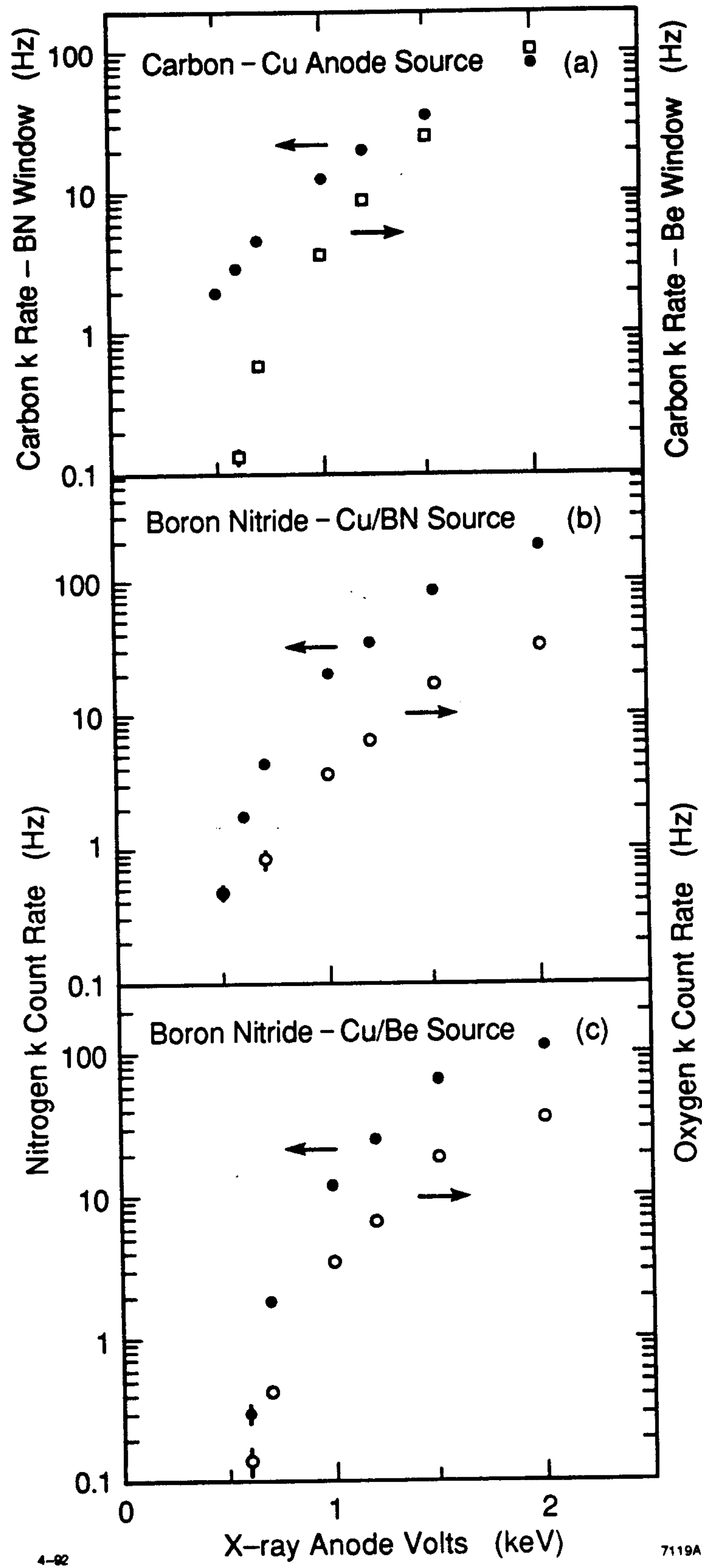
Carbon - Cu Anode Source
(a)
Carbon k Rate - BN Window (Hz)
Carbon k Rate - Be Window (Hz)
100
10
1
0.1
Boron Nitride - Cu/BN Source
(b)
100
10
1
0.1
Boron Nitride - Cu/Be Source
(c)
100
10
1
0.1
Nitrogen k Count Rate (Hz)
Oxygen k Count Rate (Hz)
0
1
2
X-ray Anode Volts (keV)
4-92
7119A7

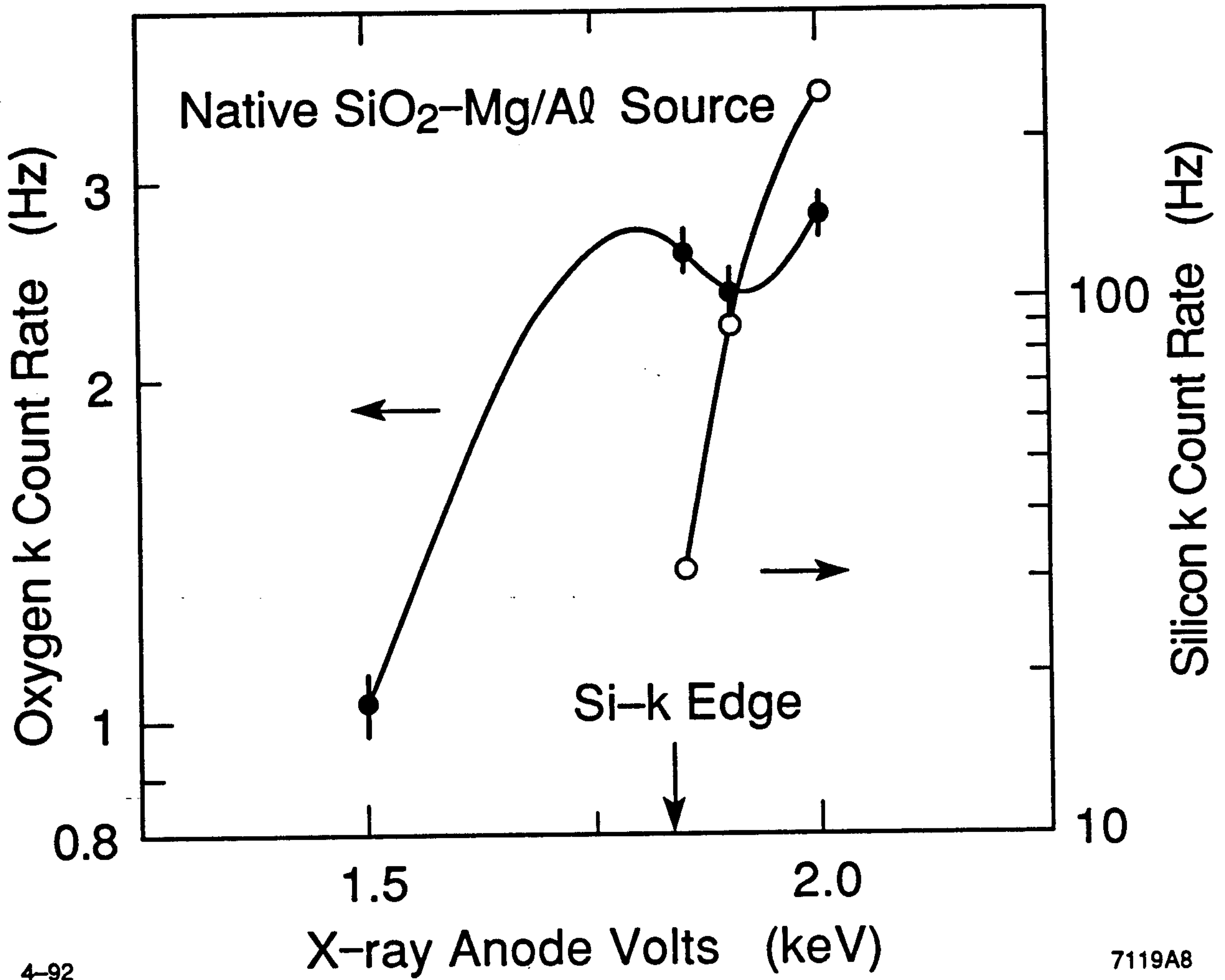
Native SiO_2–Mg/Aℓ Source
Oxygen k Count Rate (Hz)
Silicon k Count Rate (Hz)
3
2
1
0.8
100
10
Si–k Edge
1.5
2.0
X–ray Anode Volts (keV)
4–92
7119A8

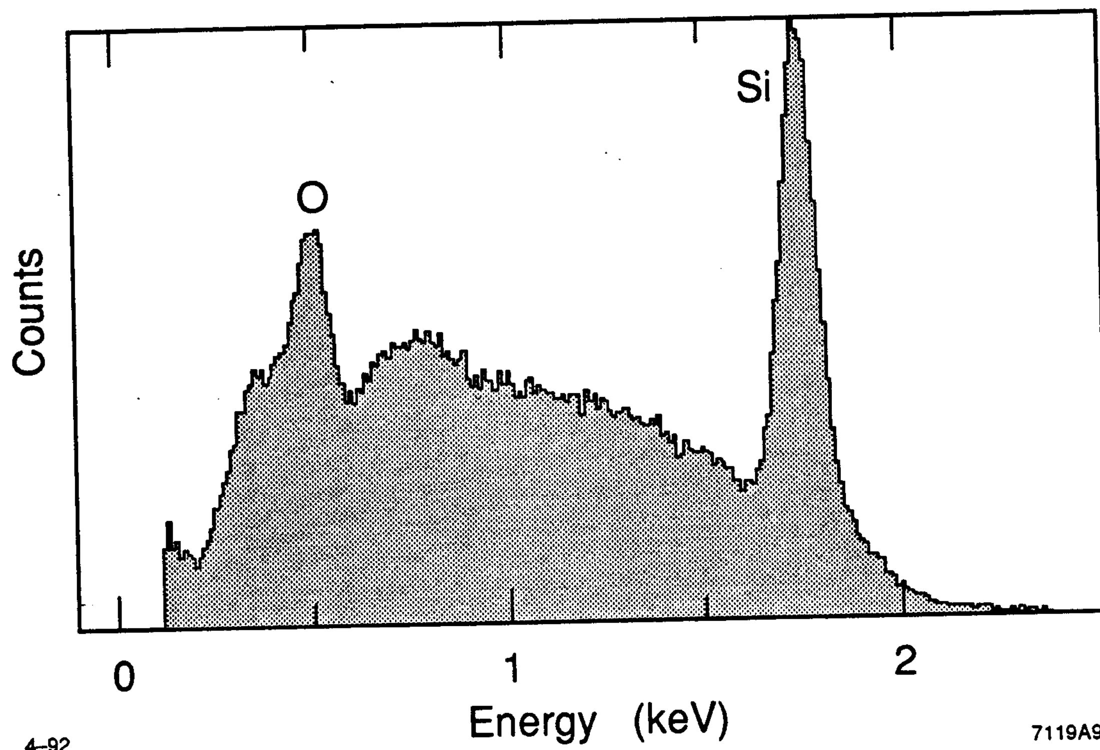

Si
O
Counts
0
1
2
Energy (keV)
4–92
7119A9

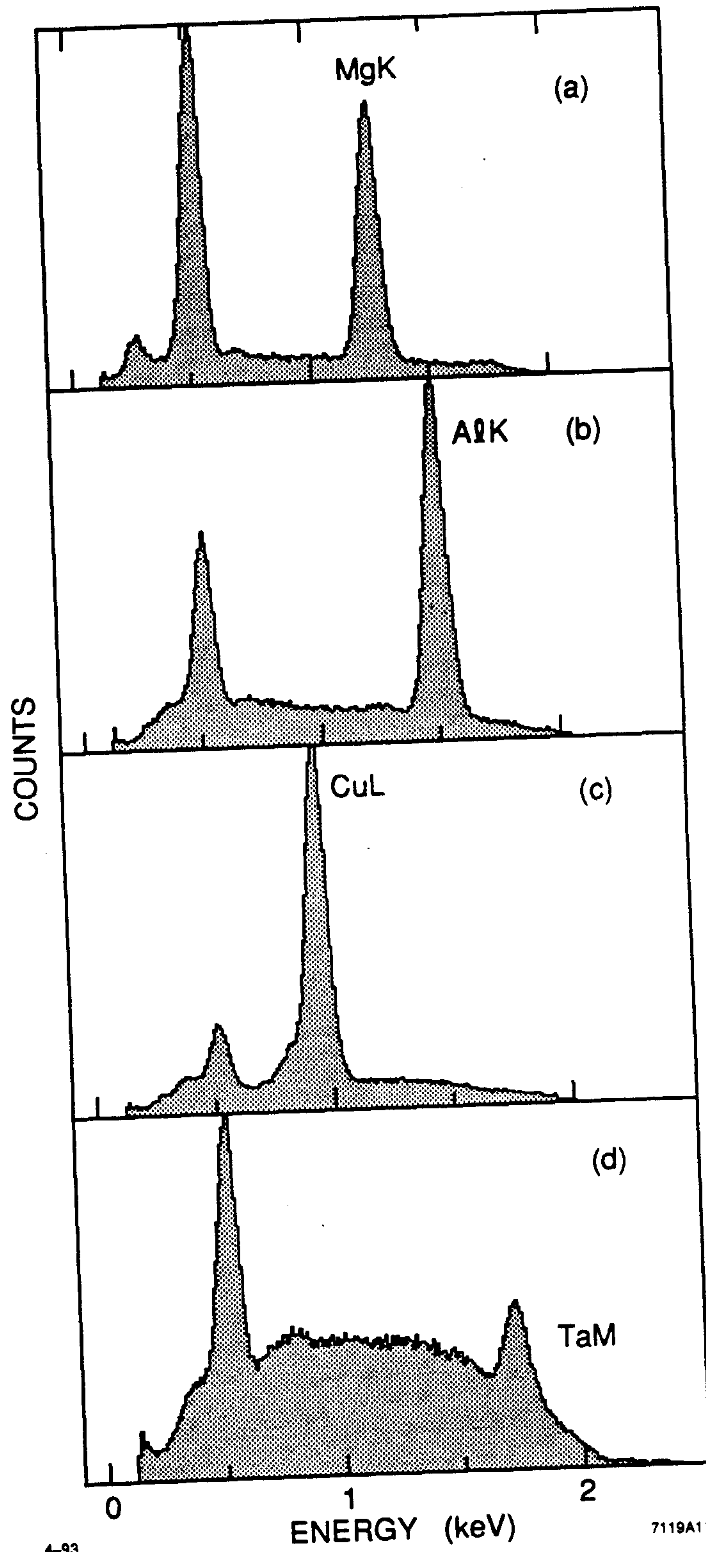
MgK
(a)
AℓK
(b)
CuL
(c)
(d)
TaM
COUNTS
0
1
2
ENERGY (keV)
4-93
7119A11

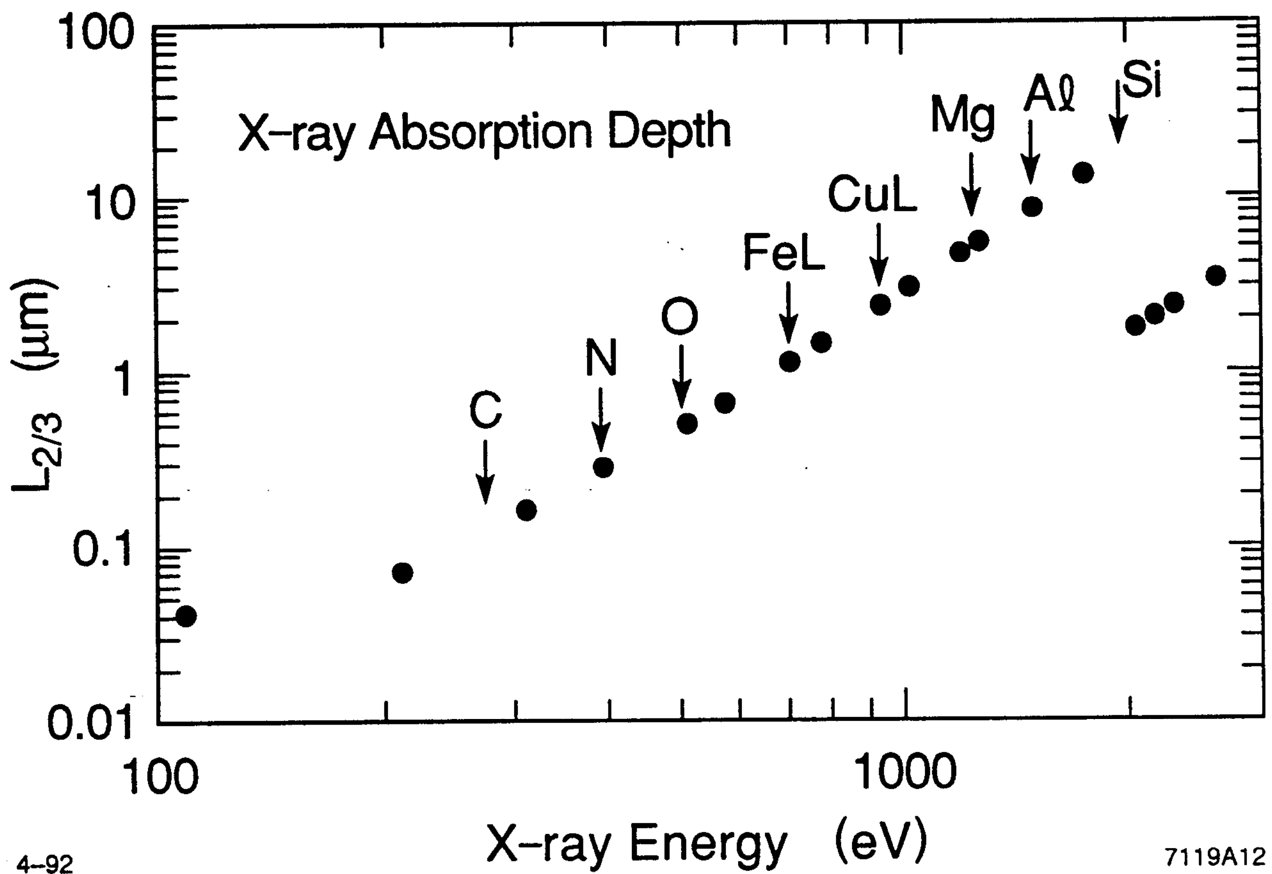
X–ray Absorption Depth
100
10
1
0.1
0.01
L2/3 (μm)
100
1000
X–ray Energy (eV)
C
N
O
FeL
CuL
Mg
Aℓ
Si
4–92
7119A12